Fluxes of energetic neutral helium atoms from the heliosheath and the IBEX Ribbon

Paweł Swaczyna, Stan Grzedzielski, and Maciej Bzowski
Space Research Centre of the Polish Academy of Sciences, Warsaw, Poland

EGU2014-223

Introduction

Full sky maps of energetic neutral hydrogen atoms (H ENA) obtained with IBEX, revealed a bright, arc-like Ribbon, which dominates over the heliosheath emission on large swaths of the sky. Potentially, the helium ENA emission could give complementary information about the heliosphere and its environment.

Helium binary interactions

Hydrogen → important charge-exchange with protons ($H^+ + H^0 \rightarrow H^0 + H^+$)
→ other: almost negligible if the energy is small $\lesssim$ 100 keV

Helium:

- three charge-states He^{2+} (α-particles), He^+ and He^0
- a number of different reactions that change charge state of He ion or atom, including ionization (ion), charge-exchange (cx), double charge-exchange between He^{2+} and He^0 (2cx)
- contributions depends on assumed conditions in plasma (different in the inner heliosheath, interstellar medium, and hot interstellar bubbles)

For energy $\lesssim$ 10 keV the mean free path (m.f.p.) against He ENA ionization is up to one order of magnitude longer than the m.f.p. of H ENA.
For assumed Local Interstellar Medium (LISM) conditions:
$n_H = 0.194$ cm^{-3}, $n_p = 0.056$ cm^{-3}, $n_{He} = 0.0153$ cm^{-3}, $n_{He^+} = 0.0096$ cm^{-3}, m.f.p. of He ENA: 7 800 AU; H ENA 870 AU at $E = 5$ keV.

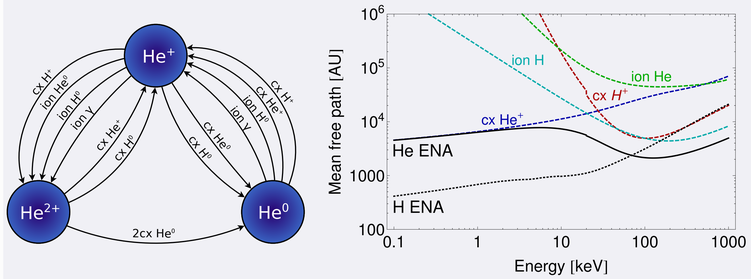

Figure 1. Left panel – diagram presenting the important binary interactions in the heliosphere and LISM. Right panel – the m.f.p. against H/He ENA ionization in the LISM. For He ENA, contributing reactions are presented by color lines.

Heliosheath signal (Grzedzielski et al. 2013 & 2014)

To asses the inner heliosheath contribution to He ENA fluxes we use a simple axisymmetrical analytical model by Suess & Nerney (1990):

- circular termination shock (TS) at 94 AU (as measured by Voyager 2)
- distance to heliopause at the Voyager 1 trajectory: 121 AU
- plasma density in the inner heliosheath 0.002 cm^{-3}
- post-termination-shock bulk plasma velocity 150 km/s
- He ion spectra consist of solar wind particles and pick-up ions (PUI)
  → PUI – assumed κ-distribution consistent with high energy Voyager data

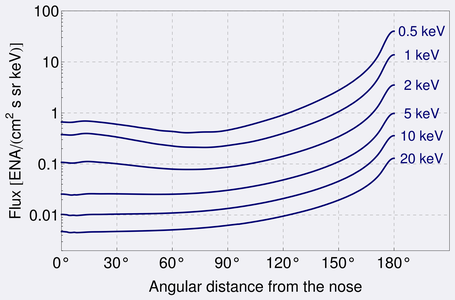

Figure 2. Simulated He ENA intensities from the inner heliosheath as functions of angular distance from the nose (the symmetry axis). For energy 100 – 200 keV the results are consistent with the HSTOF measurements.

IBEX Ribbon – two hypothetical sources (Swaczyna et al. 2014)

Secondary ENA Model

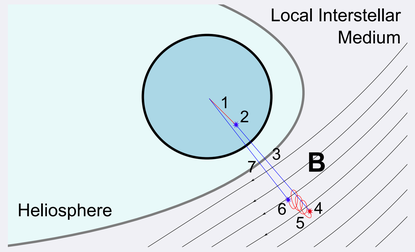

Production of ENA in the LISM just outside the heliopause in the direction where the line-of-sights are perpendicular to the direction of the magnetic field.

Extraheliospheric Model

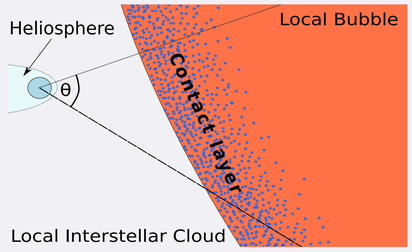

Production of ENA in the contact layer between the Local Interstellar Cloud (LIC) and a hypothetical bay of the Local Bubble (LB).

Mechanism

The solar wind ions (1) are neutralized inside the TS (2) and create a flux of primary ENA (3). The primary ENA are ionized (4) and became PUIs (5), which after subsequence neutralization (6) produce a thin disk of secondary ENA emission (7).

The neutral hydrogen and helium atoms from the LIC evaporate into the LB. Part of the suprathermal ions in the LB after neutralization on the neutrals are a source of the observed ENA. The Ribbon is a geometric effect of different integration path lengths.

Basic model

Adapted analytical model by Möbius et al. (2012) with heliolatitude dependence of the solar wind parameters (Sokół et al. 2013), the LISM densities as presented in the section "Helium binary interactions".

Adapted analytical model by Grzedzielski et al. (2010), set (4) of parameters in the plane model. Energy dependence based on the hydrogen ENA measured in the ribbon direction near the nose.

Geometry

Assumed small circle: center (λ, β)=(219.2°, 39.9°); radius 74.5°, width 15° (Funsten et al. 2013)

Governed by the extinction in the LIC, planar interface between the LIC and LB with the smallest distance in the center of the Ribbon.

Results – maps of expected He ENA flux in the two hypotheses

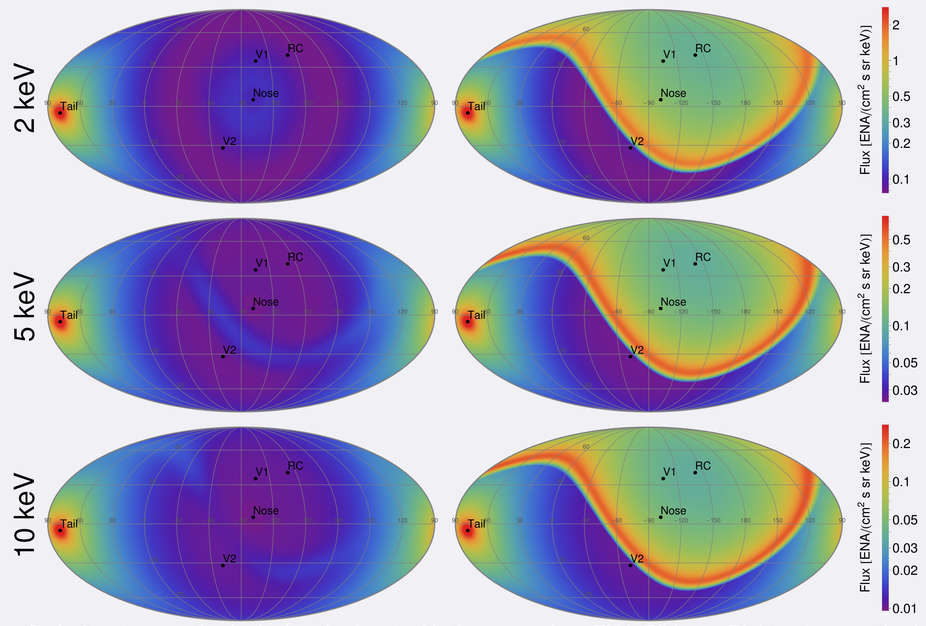

Figure 3. Left column – the heliosheath signal with the secondary ENA Ribbon. Right column – the heliosheath signal with the extraheliospheric Ribbon.

Hydrogen Ribbon – comparison between data and models

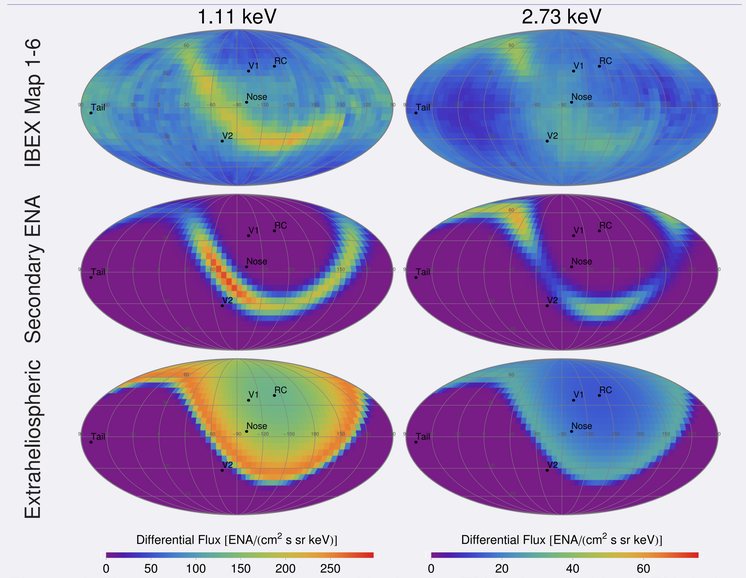

Figure 4. Comparison of the fluxes of hydrogen ENA observed by IBEX during the first 3 years (McComas et al. 2012) with the fluxes in the models of the Ribbon. The heliospheric ENA are not included in the models plots.

Conclusions – expected properties of the He ENA signal

Ratio ($E \sim 1$ keV/nuc)	Sec. ENA	Extrahel.
He-to-H ENA flux from the Ribbon	0.0001	0.01
The Ribbon-to-heliosheath He ENA flux	0.5	50

- The expected **heliospheric** signal is highly concentrated in the direction of the heliospheric **tail**: Flux(tail)/Flux(nose) $\sim 10^2$
- If observed hydrogen atoms from the Ribbon are the **secondary ENA** then observation of the He ENA signal from the Ribbon is **not likely** due to too small amount of helium in the neutral solar wind.
- If the Ribbon is produced as in the **extraheliospheric** model then the He ENA signal from the Ribbon **dominates** over the heliosheath signal except for the heliospheric tail and should be potentially easily detectable.

Outlook

- The long mean free path against ionization of **keV He ENA** in the LISM and low heliosheath signal in large part of the sky make He ENA a good candidate for **studies of the LISM structure** at distances comparable with the distance to the LIC edge (**0.05 pc** ≈ **10 000 AU**, Redfield & Linsky 2000).
- For two-dimensional sources (e.g. interfaces), also secondary ENA, i.e., produced from the ionized and then neutralized primary ENA, should give a non-negligible contribution and be included into future considerations.

References

Funsten et al. 2013, ApJ, 776, 30
Grzedzielski et al. 2010, ApJL, 715, L84
Grzedzielski et al. 2013, A&A, 549, A76
Grzedzielski et al. 2014, A&A, 563, A134
McComas et al. 2012, ApJS, 203, 1
Möbius et al. 2013, ApJ, 766, 129
Redfield & Linsky 2000, ApJ, 534, 825
Sokół et al. 2013, Solar Phys. 285, 167
Suess & Nerney 1990, JGR, 95, 6403
Swaczyna et al. 2014, ApJ, 782, 106

This work was supported by the Polish National Science Centre grant 2012-06-M-ST9-00455.

http://www.cbk.waw.pl/en
http://www.cbk.waw.pl/~pswaczyna
pswaczyna@cbk.waw.pl